Photodynamic inactivation of *Staphylococcus aureus* biofilms using a hexanuclear molybdenum complex embedded in transparent polyHEMA hydrogels

Noelia López-López,[a] Ignacio Muñoz Resta,[a] Rosa de Llanos,[b] Juan F. Miravet,[a] Maxim Mikhaylov,[c] Maxim N. Sokolov,[c] Sofía Ballesta,[d,e] Isabel García-Luque,[d,e] Francisco Galindo*[a]*

(a) Departamento de Química Inórganica y Orgánica, Universitat Jaume I, Av. Sos Baynat s/n, 12071, Castellón, Spain.

(b) Unidad Predepartamental de Medicina, Universitat Jaume I, Av. Sos Baynat s/n, 12071, Castellón, Spain.

(c) Nikolaev Institute of Inorganic Chemistry, Siberian Branch of the Russian Academy of Sciences 3 Acad. Lavrentiev Prosp., 630090 Novosibirsk, Russia.

(d) Departamento de Microbiología, Facultad de Medicina, Universidad de Sevilla, Av. De Sanchéz Pizjuán s/n, 41009, Sevilla, Spain.

(e) Red Española de Investigación en Patología Infecciosa (REIPI RD16/0016/0001), Instituto de Salud Carlos III, Madrid, Spain.

Abstract

Three new photoactive polymeric materials embedding hexanuclear molybdenum cluster $(Bu_4N)_2[Mo_6I_8(CH_3COO)_6]$ (**1**) have been synthesized and characterized by means of FTIR, TGA and emission spectroscopy. The materials are obtained in the format of transparent and thin sheets, and the formulations used to synthesize them are comprised by 2-hydroxyethylmethacrylate (HEMA), as polymerizable monomer, and ethyleneglycol dimethacrylate (EGDMA) or polyethyleneglycol dimethacrylate (PEGDMA), as crosslinkers. All the polymeric hydrogels generate singlet oxygen ($^1O_2$) upon irradiation with visible light (400-700 nm), as demonstrated by the reactivity towards two chemical traps of this reactive

species (9,10-dimethylanthracene and 1,5-dihydroxynaphthalene). Differences have been detected between the photoactive materials, probably attributable to variations in permeability to solvent and oxygen. Notably one of the materials resisted up to 10 cycles of photocatalytic oxygenation reactions of 1,5-dihydroxynaphthalene. All the three polyHEMA hydrogels doped with **1** are efficient against *S. aureus* biofilms when irradiated with blue light (460 nm). The material made with the composition 90% HEMA and 10% PEGDMA (**Mo6@Polymer-III**) is especially easy to handle, because of its flexibility, and it achieves notable levels of bacterial reductions (3 $\log_{10}$ CFU/cm^2). The embedding of **1** in crosslinked polyHEMA sheets affords a protective environment to the photosensitizer against aqueous degradation while preserving the photochemical and photo-bactericidal activity.

Introduction

Antibiotic-resistant bacteria are a great menace for modern societies since uncontrolled spreading of such pathogens can lead to serious nosocomial infections, which imply an enormous economic burden for public health systems.[1] One of the most important features of many pathogenic microorganisms is their ability to form resistant biofilms, i.e. organized macro-colonies of bacterial cells, much more difficult to eradicate than isolated bacteria in suspension.[2] It is considered, that more than 60% of microbial infections are originated by biofilms grown in surfaces.[3]

Antimicrobial photodynamic inactivation (aPDI) of microorganisms like bacteria, fungi and viruses is an attractive tool recently employed to prevent the spreading and growth of microbial pathogens. This approach implies the use of a photosentitizer, which in combination with light leads to the generation of cytotoxic species like singlet oxygen ($^1O_2$) or superoxide ($O_2^{\cdot -}$).[4-9] A great number of publications have appeared during the last years, advocating for the use of this strategy, with

emphasis in the development of materials,[10-14] especially to be used for the manufacture of healthcare-related objects.[15-17]

Currently there is a growing interest in developing new families of photosensitizers different from classical molecules like Rose Bengal, methylene blue or porphyrins / phthalocyanines, ubiquitously found in the literature and employed with great success in the past, but which are not exempt from drawbacks (photobleaching, tendency to aggregation, etc).[18] The group of hexanuclear molybdenum clusters described by the formula $[Mo_6L^i_8L^a_6]^{n-}$ (L^i and L^a are inner and apical ligands, respectively) has been receiving increasing attention due to their outstanding photophysical properties. A great number of such species have been described so far, both in solution [19–29] and immobilized in a series of supports like, for instance, polyurethane, poly(methyl methacrylate), zinc oxide and other materials. [30-43] After excitation with visible light the triplet excited state is very efficiently populated, and many of such complexes, especially the iodides (L = I), are able to emit phosphorescence in the deep-red region of the spectrum, even at room temperature. Another relevant property of this class of complexes is their ability to generate $^1O_2$ after irradiation. This reactive oxygen species is known to have great variety of applications, from oxygenation reactions[44,45] to the aforementioned elimination of pathogenic microorganisms. In this last regard, the antibacterial applications of the $\{Mo_6\}$ clusters are still far from full development. Only few cases of photo-bactericidal materials based on hexanuclear molybdenum clusters have been reported. We have shown that $(Bu_4N)_2[Mo_6I_8(CH_3COO)_6]$ (**1**) supported on macroporous and gel type cationic polystyrene is able to kill gram-positive (*Staphylococcus aureus*) and gram-negative (*Pseudomonas aeruginosa*) bacteria.[46,47] Kirakci et al. have shown that irradiated complexes of $[Mo_6I_8(OOC(CH_2)_4PPh_3)_6]Br_4$ can reduce the population of gram-positive

Enterococcus faecalis and *S. aureus*.[48] More recently, Vorotnikova et al. have shown that $(Bu_4N)_2[Mo_6I_8(CF_3(CF_2)_6COO)_6]$ used as an additive to polymer F-32L can kill *Escherichia coli, S. aureus, Salmonella typhimurium* and *P. aeruginosa* upon irradiation.[49] It must be noted that all the above mentioned investigations report bacteria in the planktonic state.

The purpose of this article is to present a series of polymeric hydrogels materials, in the format of thin polymeric films, embedding **1** as photosensitizer, capable to generate $^1O_2$ very efficiently upon irradiation, and to significantly suppress the growth of *S. aureus* biofilms. To the best of our knowledge this is the first example of use of a hexanuclear molybdenum cluster, in combination with light, to prevent the growth of a bacterial biofilm, specifically of *S. aureus*. We hope that these results will contribute to develop the field of aPDI, specifically against bacterial biofilms, and to boost the use of this new class of $\{Mo_6\}$ nanoclusters in healthcare materials, such as catheters, gloves, thermometers, or in ordinary objects, such as computer keyboards, doorknobs, and mobile phone screens.

Results and discussion

Following our previously described procedures for the preparation of polymeric hydrogel sheets hosting optically active molecules and nanoparticles,[50–56] cluster **1** (1% wt) was dissolved in three different formulations comprising monomer 2-hydroxyethylmethacryate (HEMA) and two types of crosslinkers, ethyleneglycol dimethacrylate (EGDMA) and polyethyleneglycol dimethacrylate (PEGDMA) (**Figure 1**). The aim of using different types and proportions of cross-linkers was to study the effect of these polymerizable components on the photodynamic performance of fabricated materials. According to our experience, the introduction of PEGDMA in a low percentage increases notably the permeability of the films to inorganic species such

as nitrite. In **Table 1** the three formulations employed for this study are shown. Polymers based on monomer HEMA (leading to the so-called polyHEMA materials) have been described in the literature for years due to their high water permeability and biocompatibility. For instance, they form the basis of contact lenses, orthopedic implants, and drug delivery devices.[57,58] Our aim was to develop matrices strong enough to retain **1**, but with enough permeability to allow water and O_2 to get in, and $^1O_2$ to get out of the materials. The mixtures of olefins indicated in **Table 1** (with added 1% wt of azobisisobutyronitrile, AIBN) were introduced into glass molds (see previous procedures [50–56]) and kept at 85 ºC during 15 min. This procedure induces radical polymerization, leading to the formation of transparent films of polymeric hydrogels. After mechanical removal of the molds, series of polymer films were obtained. The polymers embedding the Mo_6 cluster were named **Mo6@polymer-I**, **Mo6@polymer-II** and **Mo6@polymer-III**, whereas control materials without the photosensitizer were named simply **I**, **II** and **III**. The materials were washed and characterized by means of Fourier-transform infrared spectroscopy (FTIR), thermogravimetric analyses (TGA) and emission spectroscopy. The thickness of the films was measured, giving the averaged value of (120 ± 10) μm.

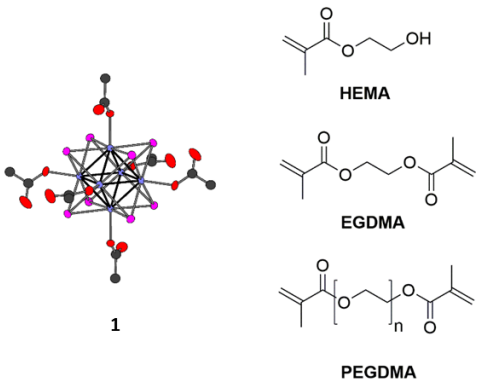

Figure 1. Structures of the octahedral cluster in $(Bu_4N)_2[Mo_6I_8(CH_3COO)_6]$ **(1)**, monomer HEMA and crosslinkers EGDMA and PEGDMA. For **1**, color codes in external ligands: red = oxygen, grey = carbon. Color code in internal atoms: pink = iodide, blue = molybdenum.

Table 1. Compositions of monomer and cross-linker mixtures leading to the polymers used in this study.

	Monomer (%wt)	Crosslinkers (%wt)		Photosensitizer
	HEMA	**EGDMA**	**PEGDMA**	**1** [(a)]
Mo6@polymer-I	67	33	-	Yes
I	67	33	-	No
Mo6@polymer-II	90	10	-	Yes
II	90	10	-	No
Mo6@polymer-III	90	-	10	Yes
III	90	-	10	No

(a) 1% wt relative to the total mass of monomer and cross-linker.

The infrared spectra of the samples showed the typical pattern of cross-linked polyHEMA materials, with a broad band around 3400 cm^{-1} corresponding to the O-H stretching in hydroxyl groups, which impart hydrophilicity to the hydrogels. Also worth of note is the disappearance of vibration at 1640 cm^{-1} corresponding to the C=C bonds in HEMA monomer and EGDMA and PEGDMA cross-linkers, as a result of the polymerization reaction. No band corresponding to the molybdenum complexes was detected, due to their low concentration in the materials (see the spectra in the **Electronic Supporting Information -ESI-** file). The samples were also analyzed by TGA, and interesting differences were found between the polyHEMA polymers containing molybdenum cluster and the corresponding controls without the photosensitizer. As it can be seen in the **ESI** file, all the six samples commonly displayed a loss of mass below 300ºC, corresponding to the decomposition of the polyHEMA structure (10% mass loss at about 250ºC; full decomposition at around 400 ºC), but the samples containing the photosensitizer do not loss the full weight of the material until 500ºC (10% mass loss occurring at about 270-280ºC). This fact would point out to some kind of additional cross-linking effect of the molybdenum cluster on

the structure of the materials, the study of which is out of the scope of this paper. Regarding the emission measurements, samples under UV excitation are emit reddish phosphorescence observable even with the naked eye (see **Figure S2**), and the spectrum of such luminescence reveals the typical broad band of emissive hexanuclear molydbenum complexes between 600 and 750 nm.[19-43,46-49] Minor differences can be found between the polymeric samples and also when compared to a solid sample of **1** and to an ethanolic solution of the photoensitizer (see **Figure 2**), probably due to different solvation environments, in agreement with the literature.[19-43,46-49] In the case of the materials here described, the presence of this emissive band confirms that the structural integrity of the photosensitizer remains intact after the polymerization reaction. Also, it could be speculated that, due to the low concentration of **1** and to the anionic nature of this photosensitizer, aggregation does not place (future microscopic studies will shed light on the distribution of **1** within these and other polyHEMA matrices).

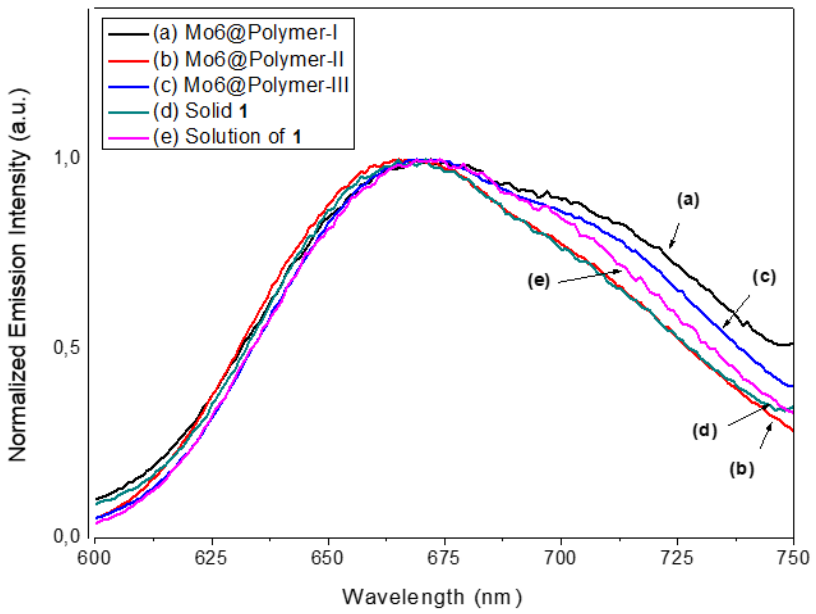

Figure 2. Normalized emission spectra of **Mo6@polymer-I**, **Mo6@polymer-II**, **Mo6@polymer-III**, **1** in ethanol solution and **1** in the solid state. λ_{exc} = 470 nm.

Next, we proceeded to study the photochemical performance of the obtained polymeric hydrogels doped with **1**. The ability of the polymeric photosensitizers to generate $^1O_2$ was checked by means of two benchmark reactions: the transformation of 9,10-dimethylanthracene (**DMA**) into an endoperoxide (DMA·O_2), and the conversion of 1,5-dihydroxynaphthalene (**DHN**) into juglone. Both reactions can be followed easily by means of UV-vis spectroscopy as it can be seen in **Figures 3** and **4**.

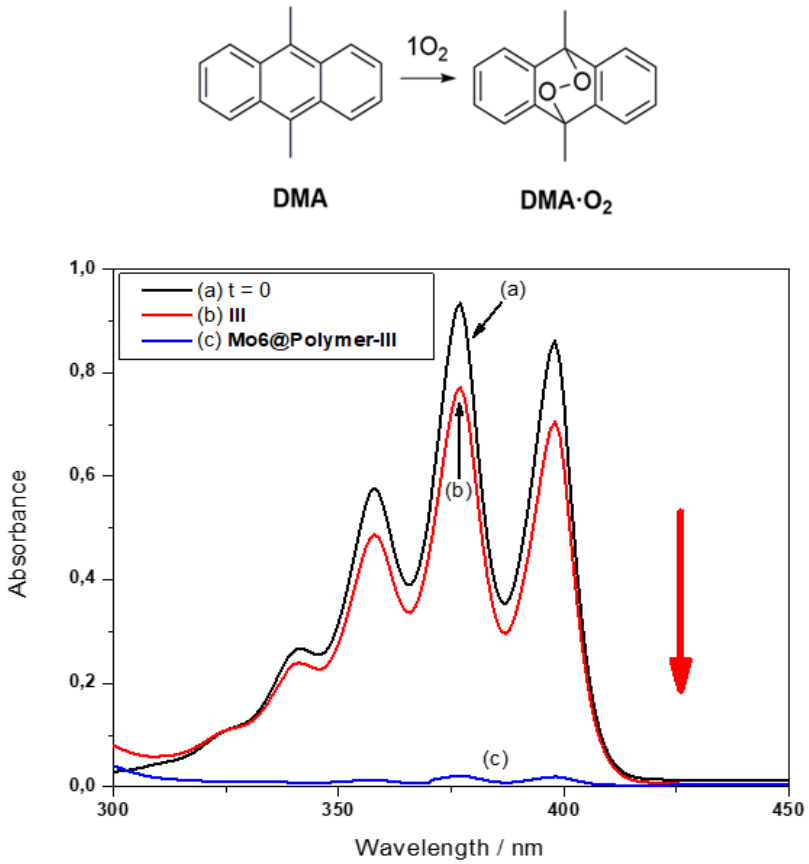

Figure 3. Up: Reaction between **DMA** and $^1O_2$ in EtOH-H_2O (1:1). Bottom: representative example of such reaction using **Mo6@polymer-III** as supported photosensitizer and **DMA** (10^{-4} M) as $^1O_2$ trap in EtOH-H_2O (1:1). (a) Initial absorption of **DMA**, (b) absorption of **DMA** after irradiation for 90 min in the presence of **III** as blank control and (c) absorption of **DMA** after irradiation for 90 min in the presence of **Mo6@polymer-III**. Light source: two white light LED lamps (11W each, 400-700 nm).

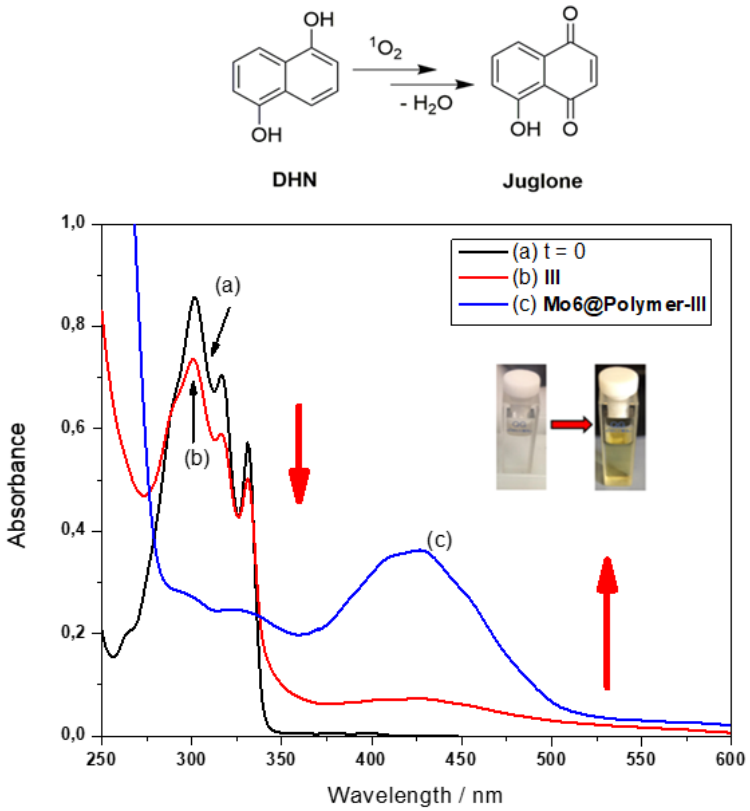

Figure 4. Up: Reaction between **DHN** and $^1O_2$ in DCM-MeOH (9:1). Bottom: representative example of such reaction using **Mo6@polymer-III** as supported photosensitizer and **DHN** (10^{-4} M) as $^1O_2$ trap in DCM-MeOH (9:1). (a) Initial absorption of **DHN**, (b) absorption of **DHN** after irradiation for 120 min in the presence of control **III** and (c) absorption of **DHN** after irradiation for 120 min in the presence of **Mo6@polymer-III**. Light source: two white light LED lamps (11W each, 400-700 nm).

The conversion of **DMA** after 90 minutes of irradiation with white light, attained with the three polymers under study, is very high, (see **Figure 5**): 83% for **Mo6@Polymer-I**, 97% for **Mo6@polymer-II** and 97% for **Mo6@polymer-III**. Also, control irradiations were conducted with empty matrices, and conversions of around 10% were obtained. It must be noted that DMA is able to generate a small amount of $^1O_2$, since some residual light can be absorbed by this probe at ca. 400 nm. But this self-oxidation reaction is much less important than the oxygenation reaction promoted by the clusters embedded on the polyHEMA films. Additionally, it must be indicated that no leaching of **1** was observed during the course of the experiments (indicated by the

lack of absorption or emission of the supernatant solutions after equilibration of films with solvent overnight).

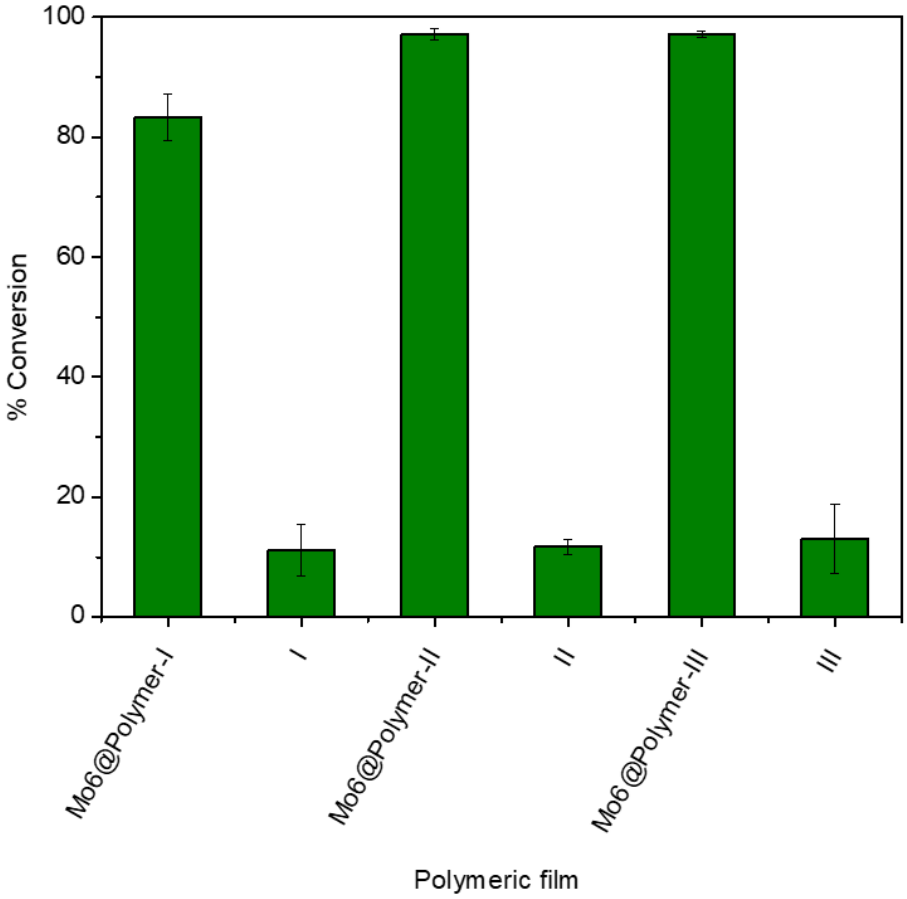

Figure 5. Conversions of **DMA** after reaction with $^1O_2$. Irradiation of polymers with white light in the presence of **DMA** (10^{-4} M). Total irradiation time is 90 min.

The photoactivity was confirmed by the photo-oxidation of **DHN** to juglone, as can be seen in **Figure 6** (again, some auto-oxidation of this substrate was observed but the amount of it is minimal in comparison with the photo-reactivity induced by the molybdenum clusters). Interestingly, the behavior of the three materials under study is slightly different, with yields of juglone, after 120 minutes of irradiation, varying from 65% (**Mo6@Polymer-I**) to 85% (**Mo6@Polymer-II**) and 92% (**Mo6@Polymer-III**). This trend might reflect the higher permeability of the hydrogel matrices made with a higher amount of HEMA (90% for **Mo6@Polymer-II** and **Mo6@Polymer-III** vs 67%

for **Mo6@Polymer-I**), in agreement with previous reports from our group dealing with sensing materials. [50–56] Especially notable is the influence of cross-linker PEGDMA, used in the manufacture of **Mo6@Polymer-III**, which is able to create a more flexible and permeable scaffold, and in consequence, to improve the photo-oxygenation efficiency of **DHN**.

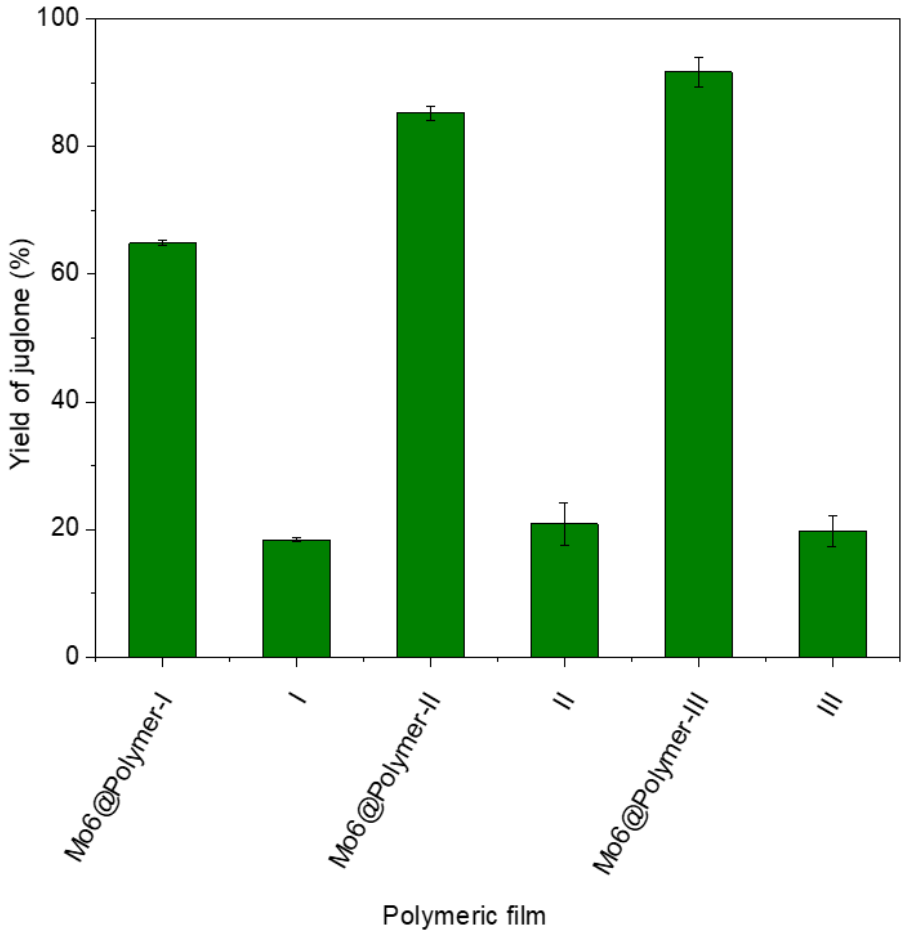

Figure 6. Yields of juglone in the reaction of **DHN** with $^1O_2$. Irradiation of polymers with white light in the presence of **DHN** (10^{-4} M). Total irradiation time is 120 min.

One of the most valuable properties of complex **1**, as earlier reported, is its high resistance to photobleaching under photochemical stress.[46,47] In order to elucidate whether this property is conserved in the polyHEMA films, a sample of **Mo6@Polymer-III** was submitted to several cycles of irradiation, using the conversion of **DHN** to juglone as test reaction. As shown in **Figure 7**, the photocatalytic ability of

Mo6@Polymer-III remarkably withstood ten cycles of irradiation without important signs of fatigue. This issue is sometimes overlooked when developing materials for aPDI, and is a characteristic that should be studied, since the materials with purported antimicrobial properties, should also show endurance after prolonged times of exposure to light. These results are in agreement with the previously reported photo-reactivity of **1** supported on polystyrene, for which no loss of activity was detected after repeated use in the photosensitized oxygenation of **DMA**.[46,47]

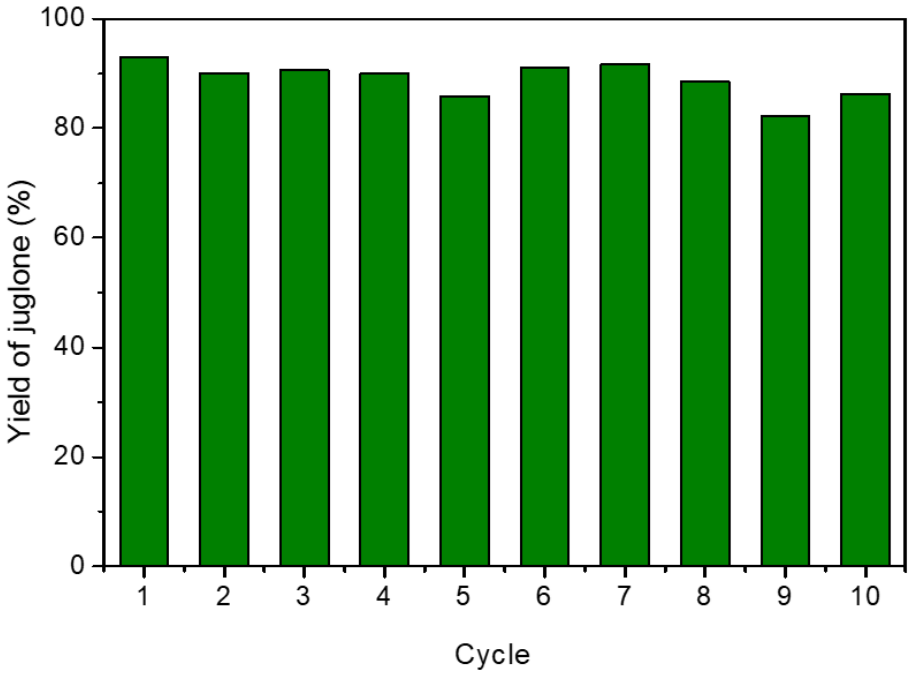

Figure 7. Yields of juglone in the reaction of **DHN** with $^1O_2$ during 10 cycles of irradiation. Irradiation of **Mo6@Polymer-III** with white light in the presence of **DHN** (10^{-4} M). For each cycle, irradiation time is 120 min.

Finally, the antimicrobial photodynamic activities of different polyHEMA hydrogels containing the {Mo_6} complexes against biofilms of *S. aureus* were evaluated (see **Figures 8 and 9**). All the polymeric films were studied in conditions of biofilm formation, and all showed antimicrobial activity, but important differences between these materials were found. The operational procedure followed to carry out this study

is the following: on small pieces of layers of **Mo6@polymer-I**, **II**, **III** (and respective control materials without photosensitizer), biofilms of *S. aureus* were allowed to grow (see experimental section). Afterwards, they were irradiated with blue light (460 nm) with a total fluence of 120 J/cm^2. Once finished the irradiation period, the biofilms were detached from the surface, and survival of the bacteria was estimated by colony counting. We are following a well-stablished methodology employing conditions that ensure the formation of a biofilm,[59] which has been used by our group in the past, with positive results.[60-62] Regarding the quantification of the bacterial survival, the colony counting methodology has proved to be a very reliable methodology.[63]

When comparing the studied polymers, it is especially remarkable the behavior of **Mo6@Polymer-III** which caused a reduction of 3.0 $\log_{10}$ CFU/cm^2 of the initial population of *S. aureus* (see in Figure 8 bacteria growing in Mueller Hinton agar plates corresponding to irradiated and non-irradiated samples of **Mo6@Polymer-III**; and see in Figure 9 the complete set of assays for all the materials). This result is of merit, since it is considered that a treatment has effective bactericidal activity when the initial inoculum is reduced by 99.9% (i.e., 3.0 $\log_{10}$ CFU/cm^2).[64] A slightly lower reduction rate was achieved with **Mo6@polymer-I** (2.8 $\log_{10}$ CFU/cm^2) while **Mo6@polymer-II** showed a reduction of 1.9 $\log_{10}$ CFU/cm^2. A practical question was also observed, which could have relevance for future studies: whereas materials **Mo6@polymer-I**, **II** were rigid and showed some tendency to break into pieces, the manipulation of **Mo6@polymer-III** was much easier due to its flexibility. Controls in the dark, both with and without **1**, showed no significant reduction of initial population. Another interesting observation is that polymers without photosensitizer (controls **I**, **II**, **III**) exposed to the light, were able to reduce the population of *S. aureus* about 1.0 to 1.5

$\log_{10}$ CFU/cm^2, but this effect could be ascribed to the well-known bactericidal effect of blue light alone.[65]

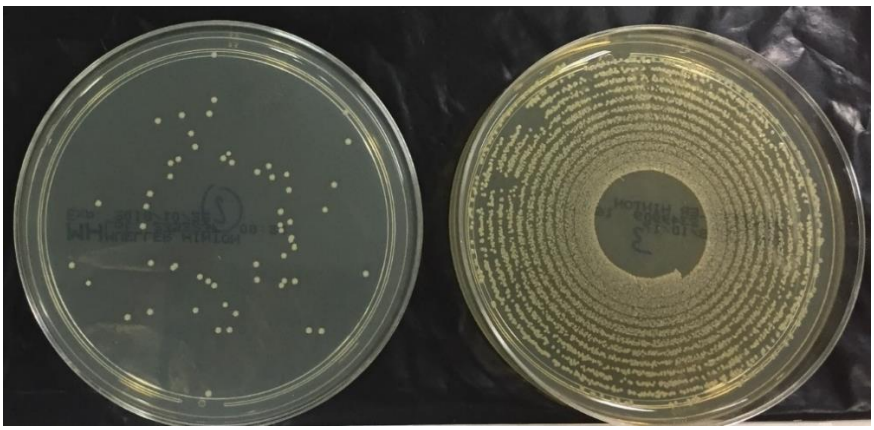

Figure 8: Representative visual example of bacteria growing in Mueller Hinton agar plates previously inoculated using a spiral plater. Left: effect of polymeric film **Mo6@polymer-III** and light. Right: effect of control without light (**Mo6@polymer-III** dark).

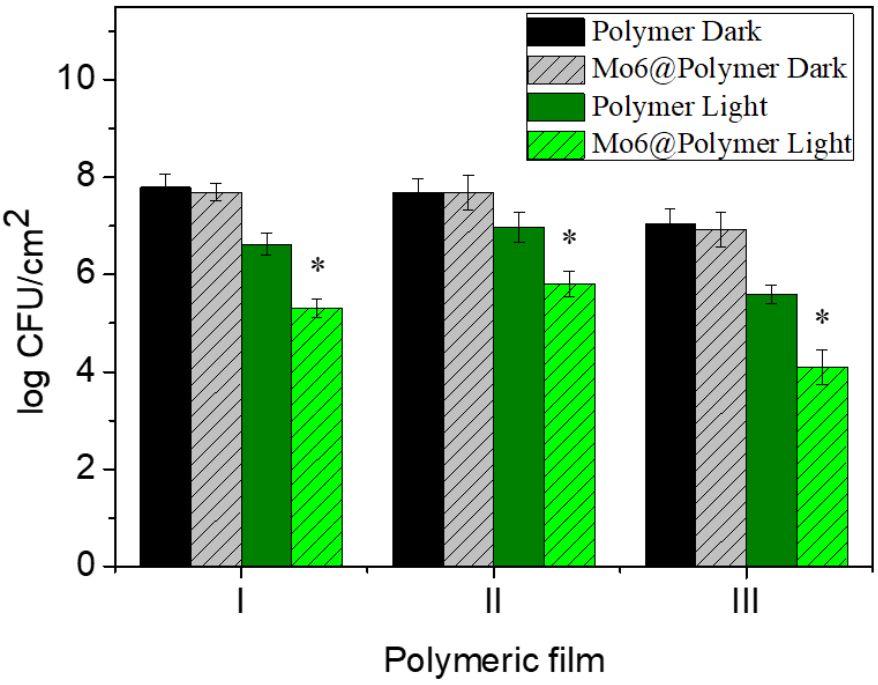

Figure 9. Antimicrobial photodynamic activity of different polyHEMA matrices containing {Mo} complexes against biofilms of *S. aureus* (n=3). * $p<0.05$

Additional measurements by scanning electron microscopy (SEM) confirmed the formation of *S. aureus* biofilms on the surface of the pHEMA hydrogels and a stricking reduction of such structures upon irradiation. Figures 10a and 10c show a biofilm formed at the surface of **Mo6@polymer-III**, at 500x and 5000x magnifications, respectively. Upon irradiation and subsequent washing, the density of bacteria is notably reduced, as it can be seen in Figures 10b (500x) and 10d (5000x). Since samples were washed before image acquisition it must be hypothesized that the irradiation weakened the extracellular matrix that holds together the bacterial biofilm. Additional SEM pictures can be found in Figure S5.

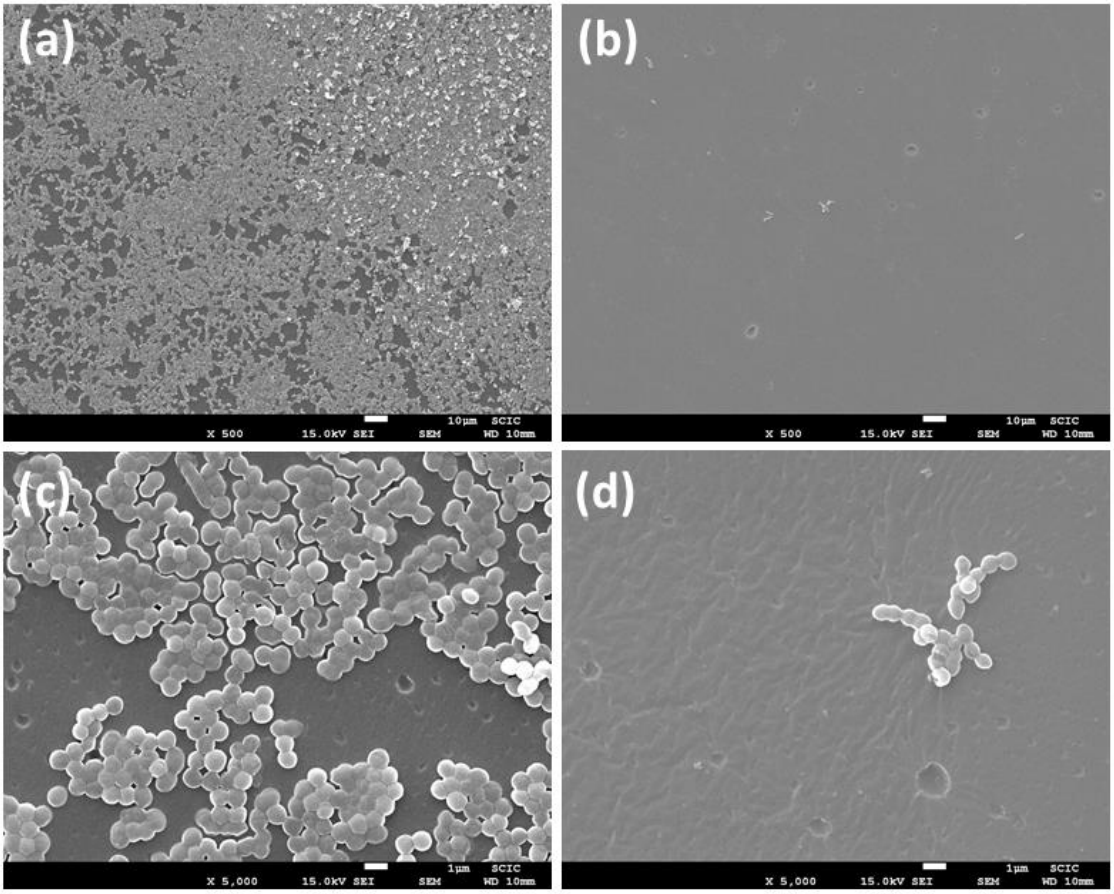

Figure 10. SEM images of hydrogel **Mo6@polymer-III** with *S. aureus* biofilm, grown in the dark (a,c) and after exposure to light (b,d). Magnification 500x (a,b; scale bar = 10 μm) and 5000x (c, d; scale bar = 1 μm). All the polymers were washed before image acquisition.

Thus, in can be concluded that the family of molybdenum clusters can be added to the list of photosensitizers successfully used to treat *S. aureus* biofilms, like, for instance, porphyrins[66] and chlorins,[67] methylene blue,[68,69] toluidine blue O[70] and hypericin.[71]

Regarding the biocidal mechanism, since the phototoxicity of {Mo} complexes is related to $^1O_2$ production, the photodynamic bactericidal activity against *S. aureus* biofilms could be related to the oxidative damage of this reactive oxygen species. Moreover, it is also known that, in addition to acting directly on bacterial cells, the products generated as a result of antimicrobial irradiations also act on the extracellular matrix of biofilm, increasing photodynamic efficiency. For instance, Beirão and coworkers have demonstrated a reduction of 81% in the polysaccharide content of the matrix of *P. aeruginosa* biofilms after treatment with a cationic photosensitizer.[70] In our case, further studies will determine the target of the $^1O_2$ generated by **1**.

In summary, three new photoactive materials embedding cluster **1** in different HEMA-based matrices have been synthesized (radical polymerization initiated by AIBN) and characterized by means of FTIR, TGA and emission spectroscopy. All the materials display excellent ability to generate $^1O_2$ upon irradiation with visible light (400-700 nm), as demonstrated by the reactivity towards two chemical traps (**DMA** and **DHN**). Differences have been detected between the photoactive materials, probably attributable to differences in permeability to solvent and oxygen. Regarding the antimicrobial activity, all the three polyHEMA hydrogels doped with **1** are efficient for inactivation of *S. aureus* biofilms, when irradiated with blue light (460 nm). The material made with the composition 90% HEMA monomer and 10% PEGDMA crosslinker (**Mo6@Polymer-III**) is especially easy to manipulate and achieves the highest levels of CFU/cm^2 reductions (3 $\log_{10}$ CFU/cm^2). The findings here reported

open the door to the development of new photoactive materials based on other hexanuclear molybdenum cluster photosensitizers and HEMA-based transparent polymeric hydrogels in the future.

Experimental part

HEMA, EGDMA, PEGDMA, AIBN were purchased in Sigma-Aldrich and used as received. Solvents were spectroscopic grade.

Preparation of photoactive films

The synthesis of cluster **1** has been described previously in the literature.[26] The synthesis of the polymeric sheets is based on previously described procedures.[50–56] In short: $(Bu_4N)_2[Mo_6I_8(CH_3COO)_6]$ (**1**) was dissolved (1% wt) in the appropriate mixture of HEMA and EGDMA or PEGDMA, following the proportions detailed in **Table 1**. Then, AIBN was added and dissolved (1% wt relative to the total mass of monomer and crosslinker). A small part of this solution was pipetted into the narrow space formed between two microscope glass slides separated by two thin lamellas at the end. In order to facilitate the later unmolding process, the glass slides were previously covered with self-adhesive PVC sheets. The system was placed in an oven at 85 °C for 15 min. After polymerization the two glass slides were separated and the film removed. Finally, the film was washed with distilled water to eliminate any unreacted material.

Steady state emission

Steady-state emission of the samples was recorded with an Agilent Cary-Eclipse spectrofluorometer at 25 °C, between 600 and 750 nm, with excitation at 470 nm. The films were supported between two microscope glass slides and placed on the corresponding solid sample holder to proceed with the measurements.

Fourier-transform infrared spectroscopy (FTIR)

FTIR microscopy was performed on a Jasco FT/IR 6200 type A with a TGS detector, between 4000 and 400 cm^{-1}.

Thermogravimetric Analyses (TGA)

Thermogravimetric analyses were performed on a TG-STDA Mettler Toledo model TGA/SDTA851e/LF/1600 coupled to a quadrupole mass spectrometer Pfeiffer Vacuum model Thermostar. Samples (6-7 mg) were heated between 25-500 °C, under air atmosphere, with a heating rate of 10°C/min.

Scanning Electron Microscopy (SEM)

Field-emission scanning electron micrographs were recorded on a JEOL 7001F microscope equipped with a CCD digital camera. The corresponding samples were placed on top of an aluminum specimen mount stub, fast-freezed with liquid nitrogen, and lyophilized overnight. The sample was then sputtered with Pt (Baltec SCD500) for 30 s and observed at 15 kV.

Benchmark model reactions to test $^1O_2$ production

Photo-oxygenation reaction of **DMA**: photochemical reactions were performed inside 10 mL sealed vials containing 50 mg of the polymeric film and 3 mL of a solution of **DMA** 10^{-4} M in EtOH-H_2O (1:1). Irradiations were carried out using two LED lamps (11 W each, Lexman, ca. 400–700 nm emission output) placed 1,5 cm away from the vial during 90 minutes, under continuous stirring. The evolution of the photoreactions was monitored over time by means of UV-vis absorption spectrophotometry (decrease of absorbance at 376 nm).

Photo-oxygenation reaction of **DHN**: photochemical reactions were performed inside 10 mL sealed vials containing 50 mg of the polymeric film and 3 mL of a solution of **DHN** 10^{-4} M in DCM-MeOH (9:1). Irradiations were carried out using two LED lamps (11 W each, Lexman, ca. 400–700 nm emission output) placed 5 cm away from the vial during 120 minutes, under continuous stirring. A chemical filter ($NaNO_2$ 0,72 M solution) between the lamps and the vial was used in this case, in order to minimize absorption of light by **DHN**. The evolution of the photoreactions was monitored over time by means of UV-vis absorption spectrophotometry (increase of absorbance at 427 nm and decrease at 300 nm).

Antimicrobial photodynamic activity against *S. aureus* biofilms

S. aureus ATCC 29213 (American Type Culture Collection, Rockville, MD, USA) was used to evaluate antimicrobial photodynamic activity of the {Mo} complexes against biofilms. To prepare bacterial inocula (protocol described in the literature[59-62]), an overnight staphylococcal culture in tryptic soy broth containing 0.25% glucose (TSB) under aerobic conditions at 37°C using a shaker incubator was adjusted to 0.5 in the McFarland scale (10^8 cells/mL) and diluted at 1:100 in TSB (final concentration: 10^6 cells/mL). Each polymeric film containing the photosensitizer (1 cm^2) (**Mo6@Polymer-I**, **Mo6@Polymer-II** or **Mo6@Polymer-III**) and its respective control (**I**, **II** or **III**) was placed in 6-well flat-bottom tissue culture plates (Cellstar®, Greiner bio-one) and 8 mL of inocula was added to each well. Plates were incubated for 24 h at 37ºC for biofilm growth.

At this time, polymeric films were taken out and washed three times with water to eliminate planktonic cells and then, they were exposed to light (LED illumination 460±10 nm) for 150 min (fluence 120 J/cm^2). Afterwards, they were washed with PBS

(buffer phosphate saline pH 7.2) and adherent bacteria were detached by sonication (40 kHz, 2 min). Samples were serially diluted in PBS and viable bacteria were determined by colony counting in Mueller Hinton Agar (MHA). Survival bacteria data are expressed as colony-forming unit/cm^2 (CFU/cm^2). In other series of experiments, polymeric films with and without {Mo} complexes were not treated with light (dark controls: **Mo6@Polymer-I**, **-II**, **-III** dark and **I**, **II**, **III** dark).

The bactericidal activity of {Mo} complexes against biofilm-forming bacteria was evaluated using the same criterion as that for bactericidal activity against planktonic bacteria; {Mo} complexes that reduced the original inoculum by 3 $\log_{10}$ CFU/mL (99.9%) were considered bactericidal.

All experiments were performed three times. The results are expressed as mean ± standard deviation. Differences between groups were compared by analysis of variance with statistical significance at $p \leq 0.05$.

For the analysis using SEM, the polymeric films were fixed for 1h in 2.5% glutaraldehyde and dehydrated in several ethanol washes (10, 25, 50, 75, and 90% for 20 min and 100% for 1h). The polymeric samples were dried overnight in a bacteriological incubator at 37ºC, and afterwards they were mounted as described previously.

Acknowledgement

Ministerio de Ciencia, Innovación y Universidades of Spain (grant RTI2018-101675-B-I00) and Universitat Jaume I (grant UJI-B2018-30) are acknowledged for their financial support. This study was also supported by Plan Nacional de I+D+i 2013-2016 and Instituto de Salud Carlos III, Subdirección General de Redes y Centros de Investigación Cooperativa, Ministerio de Ciencia, Innovación y Universidades,

Spanish Network for Research in Infectious Diseases (REIPI RD16/0016/0001) - cofounded by European Development Regional Fund “A way to achieve Europe”, Operative program Intelligent Growth 2014-2020. I.M.R. thanks the Generalitat Valenciana for a Santiago Grisolía fellowship (GRISOLIAP/2018/071). RdL is funded through a Beatriz Galindo Fellowship of the Ministerio de Educación y Formación Profesional, Spanish Government. Technical support from SCIC/UJI is also acknowledged.

Supporting information

The supporting information is available and free of charge: pictures of the irradiation setups, pictures of one representative polymeric sheet under visible and UV illumination, IR spectra for all the polymers and TGA results.

Corresponding Authors

*E-mail: igarcial@us.es

*E-mail: francisco.galindo@uji.es

ORCID ID

N. López-López: 0000-0003-2522-760X
I. Muñoz Resta: 0000-0002-1257-4517
J. F. Miravet: 0000-0003-0946-3784
M. N. Sokolov: 0000-0001-9361-4594
I. García-Luque: 0000-0003-1280-3102
S. Ballesta Mudarra: 0000-0003-3866-6804
F. Galindo: 0000-0003-0826-6084

Notes

The authors declare no competing financial interest.

Image for table of contents (TOC)

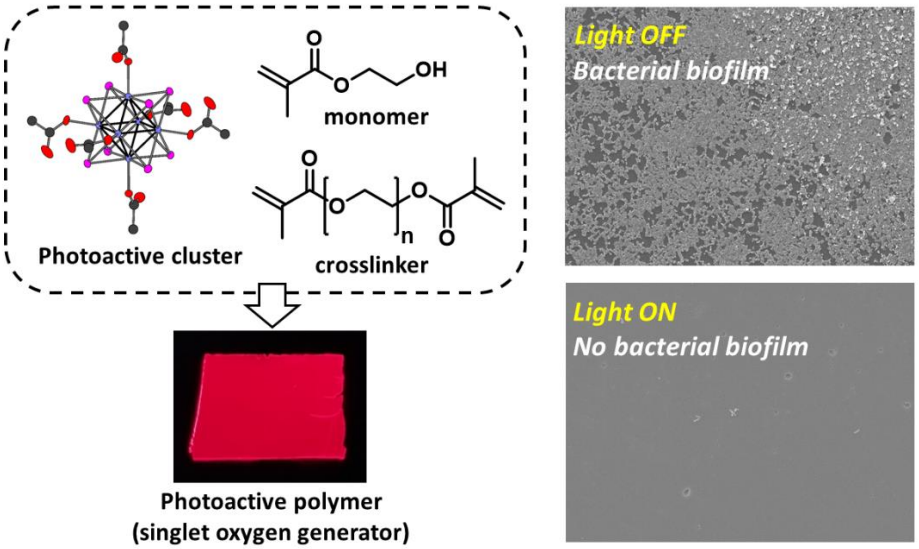

References

(1) Rice, L. B. Federal Funding for the Study of Antimicrobial Resistance in Nosocomial Pathogens: No ESKAPE. *The Journal of Infectious Diseases* **2008**, *197* (8), 1079–1081.

(2) Koo, H.; Allan, R. N.; Howlin, R. P.; Stoodley, P.; Hall-Stoodley, L. Targeting Microbial Biofilms: Current and Prospective Therapeutic Strategies. *Nature Reviews Microbiology* **2017**, *15* (12), 740–755.

(3) Lewis, K. Riddle of Biofilm Resistance. *Antimicrobial Agents and Chemotherapy* **2001**, *45* (4), 999–1007.

(4) Wainwright, M.; Maisch, T.; Nonell, S.; Plaetzer, K.; Almeida, A.; Tegos, G. P.; Hamblin, M. R. Photoantimicrobials—Are We Afraid of the Light? *The Lancet Infectious Diseases* **2017**, *17* (2), e49–e55.

(5) Wainwright, M. Synthetic, Small-Molecule Photoantimicrobials - A Realistic Approach. *Photochemical and Photobiological Sciences* **2018**, *17* (11), 1767–1779.

(6) Cieplik, F.; Deng, D.; Crielaard, W.; Buchalla, W.; Hellwig, E.; Al-Ahmad, A.; Maisch, T. Antimicrobial Photodynamic Therapy–What We Know and What We Don't. *Critical Reviews in Microbiology* **2018**, *44* (5), 571–589.

(7) Hamblin, M. R.; Abrahamse, H. Can Light-Based Approaches Overcome Antimicrobial Resistance? *Drug Development Research* **2019**, *80* (1), 48–67.

(8) Hu, X.; Huang, Y. Y.; Wang, Y.; Wang, X.; Hamblin, M. R. Antimicrobial Photodynamic Therapy to Control Clinically Relevant Biofilm Infections. *Frontiers in Microbiology* **2018**, *9*, 1–24.

(9) Jia, Q.; Song, Q.; Li, P.; Huang, W. Rejuvenated Photodynamic Therapy for Bacterial Infections. *Advanced Healthcare Materials* **2019**, *1900608*, 1–19.

(10) Mosinger, J.; Jirsák, O.; Kubát, P.; Lang, K.; Mosinger, B. Bactericidal Nanofabrics Based on Photoproduction of Singlet Oxygen. *Journal of Materials Chemistry* **2007**, *17* (2), 164–166.

(11) Feese, E.; Sadeghifar, H.; Gracz, H. S.; Argyropoulos, D. S.; Ghiladi, R. A. Photobactericidal Porphyrin-Cellulose Nanocrystals: Synthesis, Characterization, and Antimicrobial Properties. *Biomacromolecules* **2011**, *12* (10), 3528–3539.

(12) Benabbou, A. K.; Guillard, C.; Pigeot-Rémy, S.; Cantau, C.; Pigot, T.; Lejeune, P.; Derriche, Z.; Lacombe, S. Water Disinfection Using Photosensitizers Supported on Silica. *Journal of Photochemistry and Photobiology A: Chemistry* **2011**, *219* (1), 101–108.

(13) Rahal, R.; le Bechec, M.; Guyoneaud, R.; Pigot, T.; Paolacci, H.; Lacombe, S. Bactericidal Activity under UV and Visible Light of Cotton Fabrics Coated with Anthraquinone-Sensitized TiO_2. *Catalysis Today* **2013**, *209*, 134–139.

(14) Henke, P.; Kozak, H.; Artemenko, A.; Kuba, P.; Forstova, J.; Mosinger, J. Superhydrophilic Polystyrene Nanofiber Materials Generating $O_2(^1\Delta_g)$: Postprocessing Surface Modifications toward Efficient Antibacterial Effect. *ACS applied materials & interfaces* **2014**, *2*, 13007–13014.

(15) Noimark, S.; Weiner, J.; Noor, N.; Allan, E.; Williams, C. K.; Shaffer, M. S. P.; Parkin, I. P. Dual-Mechanism Antimicrobial Polymer-ZnO Nanoparticle and Crystal Violet-Encapsulated Silicone. *Advanced Functional Materials* **2015**, *25* (9), 1367–1373.

(16) Sehmi, S. K.; Noimark, S.; Bear, J. C.; Peveler, W. J.; Bovis, M.; Allan, E.; MacRobert, A. J.; Parkin, I. P. Lethal Photosensitisation of Staphylococcus Aureus and Escherichia Coli Using Crystal Violet and Zinc Oxide-Encapsulated Polyurethane. *Journal of Materials Chemistry B* **2015**, *3* (31), 6490–6500.

(17) Spagnul, C.; Turner, L. C.; Boyle, R. W. Immobilized Photosensitizers for Antimicrobial Applications. *Journal of Photochemistry and Photobiology B: Biology* **2015**, *150*, 11–30.

(18) Abrahamse, H.; R. Hamblin, M. R. New photosensitizers for photodynamic therapy. *Biochemical. Journal* **2016**, *473*, 347–364.

(19) Maverick, A. W.; Najdzionek, J. S.; MacKenzie, D.; Nocera, D. G.; Gray, H. B. Spectroscopic, Electrochemical, and Photochemical Properties of Molybdenum(II) and Tungsten(II) Halide Clusters. *Journal of the American Chemical Society* **1983**, *105* (7), 1878–1882.

(20) Grasset, F.; Molard, Y.; Cordier, S.; Dorson, F.; Mortier, M.; Perrin, C.; Guilloux-Viry, M.; Sasaki, T.; Haneda, H. When "Metal Atom Clusters" Meet ZnO Nanocrystals: A $((n\text{-}C_4H_9)_4N)_2Mo_6Br_{14}$@ZnO Hybrid. *Advanced Materials* **2008**, *20* (9), 1710–1715.

(21) Molard, Y.; Dorson, F.; Cîrcu, V.; Roisnel, T.; Artzner, F.; Cordier, S. Clustomesogens: Liquid Crystal Materials Containing Transition-Metal Clusters. *Angewandte Chemie - International Edition* **2010**, *49* (19), 3351–3355.

(22) Sokolov, M. N.; Mihailov, M. A.; Peresypkina, E. V.; Brylev, K. A.; Kitamura, N.; Fedin, V. P. Highly Luminescent Complexes $[Mo_6X_8(n\text{-}C_3F_7COO)_6]^{2-}$ (X=Br, I). *Dalton Transactions* **2011**, *40* (24), 6375–6377.

(23) Kirakci, K.; Kubát, P.; Dušek, M.; Fejfarová, K.; Šícha, V.; Mosinger, J.; Lang, K. A Highly Luminescent Hexanuclear Molybdenum Cluster - A Promising Candidate toward Photoactive Materials. *European Journal of Inorganic Chemistry* **2012**, *8* (19), 3107–3111.

(24) Sokolov, M. N.; Mikhailov, M. A.; Brylev, K. A.; Virovets, A. V.; Vicent, C.; Kompankov, N. B.; Kitamura, N.; Fedin, V. P. Alkynyl Complexes of High-Valence Clusters. Synthesis and Luminescence Properties of $[Mo_6I_8(C{\equiv}CC(O)OMe)_6]^{2-}$, the First Complex with Exclusively Organometallic Outer Ligands in the Family of Octahedral $\{M_6X_8\}$ Clusters. *Inorganic Chemistry* **2013**, *52* (21), 12477–12481.

(25) Efremova, O. A.; Vorotnikov, Y. A.; Brylev, K. A.; Vorotnikova, N. A.; Novozhilov, I. N.; Kuratieva, N. V.; Edeleva, M. V.; Benoit, D. M.; Kitamura, N.; Mironov, Y. V.; Shestopalov, M. A.; Sutherland, A. J. Octahedral Molybdenum Cluster Complexes with Aromatic Sulfonate Ligands. *Dalton Transactions* **2016**, *45* (39), 15427–15435.

(26) Mikhailov, M. A.; Brylev, K. A.; Abramov, P. A.; Sakuda, E.; Akagi, S.; Ito, A.; Kitamura, N.; Sokolov, M. N. Synthetic Tuning of Redox, Spectroscopic, and Photophysical Properties of $\{Mo_6I_8\}^{4+}$ Core Cluster Complexes by Terminal Carboxylate Ligands. *Inorganic Chemistry* **2016**, *55* (17), 8437–8445.

(27) Mikhailov, M. A.; Brylev, K. A.; Virovets, A. V.; Gallyamov, M. R.; Novozhilov, I.; Sokolov, M. N. Complexes of $\{Mo_6I_8\}$ with Nitrophenolates: Synthesis and Luminescence. *New Journal of Chemistry* **2016**, *40* (2), 1162–1168.

(28) Evtushok, D. V.; Melnikov, A. R.; Vorotnikova, N. A.; Vorotnikov, Y. A.; Ryadun, A. A.; Kuratieva, N. v.; Kozyr, K. V.; Obedinskaya, N. R.; Kretov, E. I.; Novozhilov, I. N.; Mironov, Y. V.; Stass, D. V.; Efremova, O. A.; Shestopalov, M. A. A Comparative Study of Optical Properties and X-Ray Induced Luminescence of Octahedral Molybdenum and Tungsten Cluster Complexes. *Dalton Transactions* **2017**, *46* (35), 11738–11747.

(29) Volostnykh, M. V.; Mikhaylov, M. A.; Sinelshchikova, A. A.; Kirakosyan, G. A.; Martynov, A. G.; Grigoriev, M. S.; Piryazev, D. A.; Tsivadze, A. Y.; Sokolov, M. N.; Gorbunova, Y. G. Hybrid Organic-Inorganic Supramolecular Systems Based on a Pyridine End-Decorated Molybdenum(II) Halide Cluster and Zinc(II) Porphyrinate. *Dalton Transactions* **2019**, *48* (5), 1835–1842.

(30) Fabre, B.; Cordier, S.; Molard, Y.; Perrin, C.; Ababou-Girard, S.; Godet, C. Electrochemical and Charge Transport Behavior of Molybdenum-Based Metallic Cluster Layers Immobilized on Modified n- and p-Type Si(111) Surfaces. *Journal of Physical Chemistry C* **2009**, *113* (40), 17437–17446.

(31) Molard, Y.; Labbé, C.; Cardin, J.; Cordier, S. Sensitization of Er^{3+} Infrared Photoluminescence Embedded in a Hybrid Organic-Inorganic Copolymer Containing Octahedral Molybdenum Clusters. *Advanced Functional Materials* **2013**, *23* (38), 4821–4825.

(32) Aubert, T.; Cabello-Hurtado, F.; Esnault, M. A.; Neaime, C.; Lebret-Chauvel, D.; Jeanne, S.; Pellen, P.; Roiland, C.; le Polles, L.; Saito, N.; Kimoto, K.; Haneda, H.;

Ohashi, N.; Grasset, F.; Cordier, S. Extended Investigations on Luminescent $Cs_2[Mo_6Br_{14}]@SiO_2$ Nanoparticles: Physico-Structural Characterizations and Toxicity Studies. *Journal of Physical Chemistry C* **2013**, *117* (39), 20154–20163.

(33) Amela-Cortes, M.; Garreau, A.; Cordier, S.; Faulques, E.; Duvail, J. L.; Molard, Y. Deep Red Luminescent Hybrid Copolymer Materials with High Transition Metal Cluster Content. *Journal of Materials Chemistry C* **2014**, *2* (8), 1545–1552.

(34) Efremova, O. A.; Shestopalov, M. A.; Chirtsova, N. A.; Smolentsev, A. I.; Mironov, Y. V.; Kitamura, N.; Brylev, K. A.; Sutherland, A. J. A Highly Emissive Inorganic Hexamolybdenum Cluster Complex as a Handy Precursor for the Preparation of New Luminescent Materials. *Dalton Transactions* **2014**, *43* (16), 6021–6025.

(35) Kirakci, K.; Šícha, V.; Holub, J.; Kubát, P.; Lang, K. Luminescent Hydrogel Particles Prepared by Self-Assembly of β-Cyclodextrin Polymer and Octahedral Molybdenum Cluster Complexes. *Inorganic Chemistry* **2014**, *53* (24), 13012–13018.

(36) Amela-Cortes, M.; Paofai, S.; Cordier, S.; Folliot, H.; Molard, Y. Tuned Red NIR Phosphorescence of Polyurethane Hybrid Composites Embedding Metallic Nanoclusters for Oxygen Sensing. *Chemical Communications* **2015**, *51* (38), 8177–8180.

(37) Amela-Cortes, M.; Molard, Y.; Paofai, S.; Desert, A.; Duvail, J. L.; Naumov, N. G.; Cordier, S. Versatility of the Ionic Assembling Method to Design Highly Luminescent PMMA Nanocomposites Containing $[M_6Q^i_8L^a_6]^{n-}$ Octahedral Nano-Building Blocks. *Dalton Transactions* **2016**, *45* (1), 237–245.

(38) Neaime, C.; Amela-Cortes, M.; Grasset, F.; Molard, Y.; Cordier, S.; Dierre, B.; Mortier, M.; Takei, T.; Takahashi, K.; Haneda, H.; Verelst, M.; Lechevallier, S. Time-Gated Luminescence Bioimaging with New Luminescent Nanocolloids Based on $[Mo_6I_8(C_2F_5COO)_6]^{2-}$ Metal Atom Clusters . *Physical Chemistry Chemical Physics* **2016**, *18* (43), 30166–30173.

(39) Kirakci, K.; Kubát, P.; Fejfarová, K.; Martinčík, J.; Nikl, M.; Lang, K. X-Ray Inducible Luminescence and Singlet Oxygen Sensitization by an Octahedral Molybdenum Cluster Compound: A New Class of Nanoscintillators. *Inorganic Chemistry* **2016**, *55* (2), 803–809.

(40) Solovieva, A. O.; Vorotnikov, Y. A.; Trifonova, K. E.; Efremova, O. A.; Krasilnikova, A. A.; Brylev, K. A.; Vorontsova, E. V.; Avrorov, P. A.; Shestopalova, L. V.; Poveshchenko, A. F.; Mironov, Y. V.; Shestopalov, M. A. Cellular Internalisation, Bioimaging and Dark and Photodynamic Cytotoxicity of Silica Nanoparticles Doped by $\{Mo_6I_8\}^{4+}$ Metal Clusters. *Journal of Materials Chemistry B* **2016**, *4* (28), 4839–4846.

(41) Efremova, O. A.; Brylev, K. A.; Vorotnikov, Y. A.; Vejsadová, L.; Shestopalov, M. A.; Chimonides, G. F.; Mikes, P.; Topham, P. D.; Kim, S. J.; Kitamura, N.; Sutherland, A. J. Photoluminescent Materials Based on PMMA and a Highly-Emissive Octahedral Molybdenum Metal Cluster Complex. *Journal of Materials Chemistry C* **2016**, *4* (3), 497–503.

(42) Elistratova, J.; Mukhametshina, A.; Kholin, K.; Nizameev, I.; Mikhailov, M.; Sokolov, M.; Khairullin, R.; Miftakhova, R.; Shammas, G.; Kadirov, M.; Petrov, K.; Rizvanov, A.; Mustafina, A. Interfacial Uploading of Luminescent Hexamolybdenum Cluster Units onto Amino-Decorated Silica Nanoparticles as

New Design of Nanomaterial for Cellular Imaging and Photodynamic Therapy. *Journal of Colloid and Interface Science* **2019**, *538*, 387-396.

(43) Arnau del Valle, C.; Felip-León, C.; Angulo-Pachón, C. A.; Mikhailov, M.; Sokolov, M. N.; Miravet, J. F.; Galindo, F. Photoactive Hexanuclear Molybdenum Nanoclusters Embedded in Molecular Organogels. *Inorganic Chemistry* **2019**, *58* (14), 8900–8905.

(44) Ghogare, A. A.; Greer, A. Using Singlet Oxygen to Synthesize Natural Products and Drugs. *Chemical Reviews* **2016**, *116* (17), 9994–10034.

(45) Fabregat, V.; Burguete, M. I.; Luis, S. V.; Galindo, F. Improving Photocatalytic Oxygenation Mediated by Polymer Supported Photosensitizers Using Semiconductor Quantum Dots as "Light Antennas." *RSC Advances* **2017**, *7* (56), 35154–35158.

(46) Beltrán, A.; Mikhailov, M.; Sokolov, M. N.; Pérez-Laguna, V.; Rezusta, A.; Revillo, M. J.; Galindo, F. A Photobleaching Resistant Polymer Supported Hexanuclear Molybdenum Iodide Cluster for Photocatalytic Oxygenations and Photodynamic Inactivation of: Staphylococcus Aureus. *Journal of Materials Chemistry B* **2016**, *4* (36), 5975–5979.

(47) Felip-León, C.; Arnau Del Valle, C.; Pérez-Laguna, V.; Isabel Millán-Lou, M.; Miravet, J. F.; Mikhailov, M.; Sokolov, M. N.; Rezusta-López, A.; Galindo, F. Superior Performance of Macroporous over Gel Type Polystyrene as a Support for the Development of Photo-Bactericidal Materials. *Journal of Materials Chemistry B* **2017**, *5* (30), 6058–6064.

(48) Kirakci, K.; Zelenka, J.; Rumlová, M.; Cvačka, J.; Ruml, T.; Lang, K. Cationic Octahedral Molybdenum Cluster Complexes Functionalized with Mitochondria-

Targeting Ligands: Photodynamic Anticancer and Antibacterial Activities. *Biomaterials Science* **2019**, *7* (4), 1386-1392.

(49) Vorotnikova, N. A.; Alekseev, A. Y.; Vorotnikov, Y. A.; Evtushok, D. V.; Molard, Y.; Amela-Cortes, M.; Cordier, S.; Smolentsev, A. I.; Burton, C. G.; Kozhin, P. M.; Zhu, P.; Topham, P. D.; Mironov, Y. V.; Bradley, M.; Efremova, O. A.; Shestopalov, M. A. Octahedral Molybdenum Cluster as a Photoactive Antimicrobial Additive to a Fluoroplastic. *Materials Science and Engineering: C* **2019**, *105*, 110150.

(50) Galindo, F.; Lima, J. C.; Luis, S. V.; Parola, A. J.; Pina, F. Write-Read-Erase Molecular-Switching System Trapped in a Polymer Hydrogel Matrix. *Advanced Functional Materials* **2005**, *15* (4), 541–545.

(51) Galindo, F.; Lima, J. C.; Luis, S. V.; Melo, M. J.; Jorge Parola, A.; Pina, F. Water/Humidity and Ammonia Sensor, Based on a Polymer Hydrogel Matrix Containing a Fluorescent Flavylium Compound. *Journal of Materials Chemistry* **2005**, *15* (27–28), 2840–2847.

(52) Bru, M.; Burguete, M. I.; Galindo, F.; Luis, S. v.; Marín, M. J.; Vigara, L. Cross-Linked Poly(2-hydroxyethylmethacrylate) Films Doped with 1,2-Diaminoanthraquinone (DAQ) as Efficient Materials for the Colorimetric Sensing of Nitric Oxide and Nitrite Anion. *Tetrahedron Letters* **2006**, *47* (11), 1787–1791.

(53) Burguete, M. I.; Fabregat, V.; Galindo, F.; Izquierdo, M. A.; Luis, S. v. Improved PolyHEMA-DAQ Films for the Optical Analysis of Nitrite. *European Polymer Journal* **2009**, *45* (5), 1516–1523.

(54) Fabregat, V.; Izquierdo, M. A.; Burguete, M. I.; Galindo, F.; Luis, S. V. Quantum Dot-Polymethacrylate Composites for the Analysis of NO_x by Fluorescence Spectroscopy. *Inorganica Chimica Acta* **2012**, *381* (1), 212–217.

(55) Fabregat, V.; Izquierdo, M. Á.; Burguete, M. I.; Galindo, F.; Luis, S. V. Nitric Oxide Sensitive Fluorescent Polymeric Hydrogels Showing Negligible Interference by Dehydroascorbic Acid. *European Polymer Journal* **2014**, *55* (1), 108–113.

(56) Fabregat, V.; Burguete, M. I.; Galindo, F.; Luis, S. v. Influence of Polymer Composition on the Sensitivity towards Nitrite and Nitric Oxide of Colorimetric Disposable Test Strips. *Environmental Science and Pollution Research* **2017**, *24* (4), 3448–3455.

(57) Atzet, S.; Curtin, S.; Trinh, P.; Bryant, S.; Ratner, B. Degradable Poly(2-hydroxyethyl Methacrylate)-Co-Polycaprolactone Hydrogels for Tissue Engineering Scaffolds. *Biomacromolecules* **2008**, *9* (12), 3370–3377.

(58) Galperin, A.; Smith, K.; Geisler, N. S.; Bryers, J. D.; Ratner, B. D. Precision-Porous PolyHEMA-Based Scaffold as an Antibiotic-Releasing Insert for a Scleral Bandage. *ACS Biomaterials Science and Engineering* **2015**, *1* (7), 593–600.

(59) de Melo, W. C. M. A.; Avci, P.; Nóbrega de Oliveira, M.; Gupta, A.; Vecchio, D.; Sadasivam, M.; Chandran, R.; Huang, Y. Y.; Yin, R.; Perussi, L. R.; Tegos, G. P.; Perussi, J. R.; Dai, T.; Hamblin, M. R. Photodynamic Inactivation of Biofilm: Taking a Lightly Colored Approach to Stubborn Infection. *Expert Reviews in Anti-Infective Therapy* **2013**, *11* (7), 669-693.

(60) García, I.; Ballesta, S.; Gilaberte, Y.; Rezusta, A.; Pascual, A. Antimicrobial photodynamic activity of hypericin against methicillin-susceptible and resistant *Staphylococcus aureus* biofilms. *Future Microbiol*ogy **2015**, *10*, 347-356.

(61) Pérez-Laguna, V.; Pérez-Artiaga, L.; Lampaya-Pérez, V.; García-Luque, I.; Ballesta, S.; Nonell, S.; Paz-Cristobal, M. P.; Gilaberte, Y.; Rezusta, A. Bactericidal Effect of Photodynamic Therapy, Alone or in Combination with Mupirocin or Linezolid, on *Staphylococcus aureus*. *Frontiers in Microbiology* **2017**, *8*, 1002.

(62) Pérez-Laguna, V.; García-Luque, I.; Ballesta, S.; Pérez-Artiaga, L,; Lampaya-Pérez, V.; Samper, S., Soria-Lozano, P.; Rezusta, A.; Gilaberte, Y. Antimicrobial photodynamic activity of Rose Bengal, alone or in combination with Gentamicin, against planktonic and biofilm *Staphylococcus aureus*. *Photodiagnosis and Photodynamic Therapy* **2018**, *21*, 211-216.

(63) Bankier, C.; Cheong, Y.; Mahalingam, S.; Edirisinghe, M.; Ren, G.; Cloutman-Green, E.; Ciric, L. A comparison of methods to assess the antimicrobial activity of nanoparticle combinations on bacterial cells. *PloS ONE* **2018**, 13 (2), e0192093.

(64) Clinical and Laboratory Standards Institute. Performance Standards for Antimicrobial Susceptibility Testing, CLSI M100-28th edition, Clinical and Laboratory Standards Institute, Wayne, PA (2013).

(65) Dai, T.; Gupta, A.; Murray, C. K.; Vrahas, M. S.; Tegos, G. P.; Hamblin, M. R. Blue Light for Infectious Diseases: Propionibacterium Acnes, Helicobacter Pylori, and Beyond? *Drug Resistance Updates* **2012**, *15* (4), 223–236.

(66) Beirão, S.; Fernandes, S.; Coelho, J.; Faustino, M. A. F.; Tomé, J. P. C.; Neves, M. G. P. M. S.; Tomé, A. C.; Almeida, A.; Cunha, A. Photodynamic Inactivation

of Bacterial and Yeast Biofilms with a Cationic Porphyrin. *Photochemistry and Photobiology* **2014**, *90* (6), 1387-1396.

(67) Dai, T.; Tegos, G. P.; Zhiyentayev, T.; Mylonakis, E.; Hamblin, M. R. Photodynamic Therapy for Methicillin-Resistant Staphylococcus Aureus. *Lasers in Surgery and Medicine* **2010**, *42* (1), 1–14.

(68) Pereira, C. A.; Romeiro, R. L.; Costa, A. C. B. P.; MacHado, A. K. S.; Junqueira, J. C.; Jorge, A. O. C. Susceptibility of Candida Albicans, Staphylococcus Aureus, and Streptococcus Mutans Biofilms to Photodynamic Inactivation: An in Vitro Study. *Lasers in Medical Science* **2011**, *26* (3), 341–348.

(69) Gad, F.; Zahra, T.; Hasan, T.; Hamblin, M. R. Effects of Growth Phase and Extracellular Slime on Photodynamic Inactivation of Gram-Positive Pathogenic Bacteria. *Antimicrobial Agents and Chemotherapy* **2004**, *48* (6), 2173–2178.

(70) Sharma, M.; Visai, L.; Bragheri, F.; Cristiani, I.; Gupta, P. K.; Speziale, P. Toluidine Blue-Mediated Photodynamic Effects on Staphylococcal Biofilms. *Antimicrobial Agents and Chemotherapy* **2008**, *52* (1), 299–305.

(71) Engelhardt, V.; Krammer, B.; Plaetzer, K. Antibacterial Photodynamic Therapy Using Water-Soluble Formulations of Hypericin or MTHPC Is Effective in Inactivation of Staphylococcus Aureus. *Photochemical and Photobiological Sciences* **2010**, *9* (3), 365–369.